Original Article

Prognostic value of *GARS* in bladder cancer and its role in the tumor microenvironment

Kaifei Chen, Shuaiqi Chen, Shangrong Wu, Guangyu Sun, Yuchen Jiang, Ranlu Liu

Department of Urology, Tianjin Medical University General Hospital, Tianjin, China

Contributions: (I) Conception and design: K Chen; (II) Administrative support: R Liu; (III) Provision of study materials or patients: K Chen, S Chen; (IV) Collection and assembly of data: K Chen, S Chen, S Wu; (V) Data analysis and interpretation: G Sun; (VI) Manuscript writing: All authors; (VII) Final approval of manuscript: All authors.

Correspondence to: Ranlu Liu, MD, PhD. Department of Urology, Tianjin Medical University General Hospital, 1543 Anshan Road, Heping District, Tianjin 300052, China. Email: ranluliu@126.com.

Background: Bladder cancer (BC), as a common type of cancer, has a poor prognosis, also some common invasive prognostic or therapeutic markers are difficult to obtain, which makes further treatment of BC difficult. Glycyl-tRNA synthetase (*GARS*), as one of the aminoacyl-tRNA synthetases that charge tRNAs with their cognate amino acids, has been identified as a target in many diseases, including tumors.

Methods: Bioassay analysis revealed that *GARS* was in high expression in most cancer tissues. The expression of *GARS* gene in BC tissues could assess the prognosis of BC patients, and the expression in urinary extracellular vesicles (uEVs) of patients was positively correlated with the expression in tissues. In addition to this, we analyzed *GARS*-related differential gene expression, copy number variation (CNV) and mutation profiles, potential biological functions, immune cell infiltration and drug sensitivity. *In vivo* and *vitro* tumorigenic experiments were performed to validate the function of *GARS*. Single-cell data were used to further analyze its role in the microenvironment.

Results: In our study, we found that *GARS* was highly expressed in 30 cancer tissues including BC, and high *GARS* expression was negatively correlated with the prognosis of BC patients. To address this phenomenon, we analyzed the differential genes between high and low *GARS* groups by enrichment analysis, and identified the biological signaling pathways that were mainly enriched for their functions, and found that the enrichment was found in immune-related signaling pathways and regulation of cell-cell adhesion. Then we found that *GARS* was positively associated with immune cell infiltration in BC, and some common immune checkpoints were significantly overexpressed in the *GARS*-high group. Besides, we found that *GARS* was enriched in myofibroblasts in the tumor microenvironment, and the enrichment was positively correlated with epithelial-mesenchymal transition (EMT)-related genes. This study also showed a positive correlation between *GARS* and BC RNA stemness. Patients in the *GARS*-high group had considerably higher rates of *P53* and Titin (*TTN*) mutations than those in the *GARS*-low group. Drug Sensitivity analysis screened for drugs that were more sensitive to *GARS*-high patients. Further, we found that knockdown of *GARS* significantly inhibited the proliferation, migration and invasion ability both *in vivo* and *in vitro*. Finally, we found that in patients with high *GARS* the expression in uEVs was also at a high level.

Conclusions: In summary, this study provided evidence that *GARS* can be used as a prognostic and therapeutic marker for BC, we can detect *GARS* in uEVs instead of tissue, to provide a new, simple, noninvasive way to obtain prognostic and therapeutic markers for BC patients.

Keywords: Bladder cancer (BC); GARS; urinary extracellular vesicles (uEVs); myofibroblast; prognosis

Submitted Nov 20, 2023. Accepted for publication Apr 28, 2024. Published online Jun 27, 2024.
doi: 10.21037/tcr-23-2148
View this article at: https://dx.doi.org/10.21037/tcr-23-2148

Introduction

Bladder cancer (BC) is the 10th most common form of cancer worldwide, with an estimated 549,000 new cases and 200,000 deaths in 2018 and most BC patients have a poor prognosis (1). Conventional therapies such as maximal surgical resection, chemical drug perfusion in bladder and chemotherapy of cisplatin are considered to be the best available therapeutic approaches (2). Immunotherapy has now become a major strategy for the treatment of solid tumors. Five drugs have been approved by Food and Drug Administration (FDA) for metastatic urothelial cancer including three programmed cell-death protein 1 (PD-1) inhibitors and two programmed cell-death ligand 1 (PD-L1) inhibitors in patients who have progressed during or after platinum-based therapy and achieved better treatment (3). Glycyl-tRNA synthetase (*GARS*) is critical for charging glycine onto cognate tRNA molecules and is required for protein synthesis in the mitochondria and the cytosol. The human GARS protein consists of an N-terminal WHEPTRS domain, a catalytic domain interspersed by three insertion domains and a C-terminal anticodon-binding domain (4). As the research progresses, the study of *GARS* in tumors is gradually enriched.

Khosh Kish *et al.* demonstrated that *GARS* expression is associated with prostate cancer progression and its inhibition decreases migration, and invasion *in vitro* (5). Wang *et al.* showed that *GARS* is implicated in poor survival and immune infiltration of hepatocellular carcinoma (HCC). *GARS* depletion inhibits HCC cell proliferation and cell cycle progression and promotes apoptosis *in vitro*. *GARS* overexpression promotes growth, reduces xenograft apoptosis and enhances $CD206^{+}$ tumor-associated macrophage (TAM) infiltration *in vivo* (6). And the prognostic model constructed based on cancer RNA expression also involves *GARS* (7). The apoptotic activities of naked *GARS* and *GARS*-extracellular vesicles (*GARS*-EVs) had been comparatively evaluated using different cancer cell lines. Of the 15 tested cancer cell lines, *GARS* and *GARS*-EVs promoted apoptosis in 9 and 13 cancer cell lines, respectively. Although Xu *et al.* found that *GARS* enhances DNA synthesis and promotes cell proliferation in BC cell lines by activating pentose phosphate pathway enzymes (8). However, the studies of *GARS* in BC tumor microenvironment (TME) and the prognostic value in urine are still lacking. Epithelial-mesenchymal transition (EMT), a biological process by which epithelial cells are transformed into cells with a mesenchymal phenotype through specific programs, plays an important role in cancer progression.

In this study, we investigated the expression of *GARS*, the mechanism of aberrant *GARS* expression, the correlation of *GARS* levels with clinic pathological features, prognosis and immune infiltration, and the signaling pathways and biological processes that *GARS* may affect in BC. And we explored the expression of *GARS* in the TME and its effect on EMT. In addition, we examined urinary extracellular vesicles (uEVs) from patients with BC and found that *GARS* expression in uEVs had the same trend as that was shown in tissues. Our study suggests that *GARS* could be used as a prognostic and therapeutic target for BC. We present this article in accordance with the MDAR reporting checklist (available at https://tcr.amegroups.com/article/view/10.21037/tcr-23-2148/rc).

Highlight box

Key findings

- The lower expression of glycyl-tRNA synthetase (*GARS*) was closely associated with a better prognosis for bladder cancer (BC) patients.
- *GARS* could be a target for prognosis prediction and treatment of BC patients.
- Tumor microenvironment shows that *GARS* is enriched in myofibroblasts and is involved in the progression of non-muscle invasive BC to muscle invasive BC by regulating epithelial-mesenchymal transition.
- Patients with high *GARS* the expression in urinary extracellular vesicles (uEVs) was also at a high level.

What is known and what is new?

- *GARS* encodes glycyl-tRNA synthetase, one of the aminoacyl-tRNA synthetases that charge tRNAs with their cognate amino acids. The encoded enzyme is an (alpha)2 dimer which belongs to the class II family of tRNA synthetases. It has been shown as a target of autoantibodies in human autoimmune diseases, polymyositis or dermatomyositis.
- We have analyzed *GARS* not only from the view of tumor prognosis, but also explored the information in its microenvironment. Due to the specificity of BC, we added the study of *GARS* in urine.

What is the implication, and what should change now?

- *GARS* can be used as a prognostic and therapeutic marker for BC, we can detect *GARS* in uEVs instead of tissue, to provide a new, simple, noninvasive way to obtain prognostic and therapeutic markers for BC patients.

Methods

Data acquisition

This study collected BC data from Dataset sets consisting of The Cancer Genome Atlas program (TCGA, n=407), while The TCGA Dataset obtained from University of California Santa Cruz (USCS) Xena (http://xenabroswer.net/hub), included the information of copy number, somatic mutation, DNA methylation. Meanwhile, GSE13507 was used to validate the prognostic value of *GARS* and all samples for single-cell analysis were obtained from the National Center for Biotechnology Information Gene Expression Omnibus (GEO) Dataset. Single-cell sequencing on tumor-infiltrating cells of four patients with full type cells was performed with GSE211388. The pathologic type of all patients was uroepithelial carcinoma, including three cases of muscle invasive bladder cancer (MIBC) (one with lymph node metastasis) and one case of non-muscle invasive bladder cancer (NMIBC). For the gene expression profiles across all tumor samples and paired normal tissues, the Gene Expression Profiling Interactive Analysis web server (http://gepia.cancer-pku.cn/detail.php) was used.

Analysis of the relationships between GARS, prognosis, methylation, single nucleotide polymorphism (SNP), DNA stemness score (DNAss), RNA stemness score (RNAss) and clinical phenotype

Two indicators—overall survival (OS) and progression-free survival (PFS)—were selected to study the relationship between *GARS* expression and patient prognosis using the Kaplan-Meier method and Cox regression. Survival curves were analyzed and the plots were produced by the R packages "survival" and "survminer". RNAss and DNAss of cuproptosis-associated genes were presented using the R packages "limma" and "corrplot". Spearman's test was also used during the process.

Differential expression and functional exploration of genes

Samples were divided into high and low expression groups according to the median *GARS* expression. Analysis of variance was performed using the "limma" package, taking $|\log \text{fold change (FC)}| \geq 1$, $P<0.05$. Package "clusterprofiler" was used on all differential genes to perform Gene Ontology (GO) and Kyoto Encyclopedia of Genes and Genomes (KEGG) pathway enrichment analysis. Using Fisher's exact test, those with P values less than 0.05 were regarded as significant indicators.

For human experiments: the study was conducted in accordance with the Declaration of Helsinki (as revised in 2013). The study was approved by the Medical Ethics Committee of the Second Hospital of Tianjin Medical University, Tianjin, China (KY2023K185).

For animal experiments: experiments were performed under a project license (No. JCPD20221018028) granted by Animal Ethics Committee of the Second Hospital of Tianjin Medical University, Tianjin, China (JCPD20221018028), in compliance with China animal experiments guidelines for the care and use of animals.

Differential analysis of immune cell infiltration, immune function, and immune checkpoint function

The gene set variation analysis (GSVA) package was used for single-sample gene set enrichment analysis (ssGSEA) analysis to obtain a Hallmark gene set score and bulk RNA-seq data were used to analyse *GARS*-associated immune cell subsets (9). We utilized ssGSEA technique to quantify relative infiltration levels of 28 immunological cells in BC samples. The 28 immunological invading cells had significantly varying expression levels. The "ggplot2" was utilized for visualization after 28 immunological infiltrating cells and hub genes were subjected to Spearman correlation analysis. LAG3, PDL1, PD1, TIGIT, CTLA4, VISTA, BTLA and TIM3 were used as common immune checkpoints to see the relationship between *GARS* and immunity.

Single-cell data processing

Raw data were converted into a Seurat object by the R package "Seurat" (v 3.1.2) (10). In GSE211388, cells whose percentages of ribosomes or percentage of mitochondria are less than 25 or single cells with less than 200 genes detected were considered low-quality cells and were removed. In order to eliminate potential doublets, single cells with over 5,000 genes detected were also filtered out. 35,388 single cells remained. Samples that did not contain $CD45^-$ were removed. Finally, data from four example patients were saved that contained all $CD45^+$ and $CD45^-$ cells from the four patients, 23,519 single cells remained.

After quality control, the Seurat object was normalized by the function SCTransform of the "Seurat" package. Since samples were processed and sequenced in batches, their origin tissue was used to remove the potential batch effect. In

this progress, the top 2,000 variable genes were used to create potential anchors with the FindIntegration Anchors function of "Seurat". Subsequently, the Harmony function was used to integrate data and merge a new matrix with 2,000 features, in which potential batch effect was regressed out.

To reduce the dimensionality of the scRNA-Seq dataset, principal component analysis (PCA) was performed on an integrated data matrix. With the elbow plot function of Seurat, the top 30 principal components (PCs) were used to perform the downstream analysis. The main cell clusters were identified with the FindClusters function offered by Seurat, with resolution set as default (GSE211388, res 0.1), and then they were visualized with 2D UMAP Plots (11).

Predicting anti-cancer drug response

To evaluate the ability of the *GARS* to predict the chemotherapeutic response, the half-maximal inhibitory concentration (IC50) of common chemotherapeutic drugs was first calculated in the BC samples, using the "pRRophetic" package in R software. The Wilcoxon rank test was then used to compare the difference in IC50 between the low- and high-*GARS* groups.

The Human Protein Atlas (THPA)

Information on GARS protein expression in BC versus normal samples was selected from THPA database (http://www.proteinatlas.org/). The antibody information is HPA019097. Samples' ids for normal bladder tissue are 3184, 3497 and 3517. Patients' ids for BC tissue are 1871, 2031, 2053, 2802 and 3265.

Cell lines and lentivirus infection

A normal human bladder uroepithelium cell line (SV-HUC-1) and two BC cell lines (5637 and T24) were obtained from The Cell Bank of Chinese Academy of Sciences (Shanghai, China). SV-HUC-1, T24 and 5637 were cultured in DMEM (Gibco, Carlsbad, CA, USA). All culture media contained 1% penicillin/streptomycin and 10% fetal bovine serum (FBS, Gibco). The cells were incubated in humidified air at 37 ℃ with 5% CO_2.

Three human siRNA sequences (si*GARS*-1, 5'-TGGAAGAAGTTGTTCCGAATGTAAT-3', si*GARS*-2, 5'-GACAAATTTGCTGACTTCATGGTGA-3') and negative control siRNA (siNC, 5'-GACTTTAGTCGTTCAGTACGAATGA-3') were cloned in pLKO.1-puro vector to endogenously down-regulate *GARS*. For lentiviral production, 293T cells were transfected with the lentiviral vector along with packaging plasmids using Lipofectamine 2000 (Invitrogen, Shanghai, China). Culture media was collected, pooled and filtered at 48 hours and 72 hours after transfection. Then, the indicated lentivirus was used to infect the BC cell lines.

Western blotting

Proteins were separated from cell lines 5637 and T24 utilizing radio-immunoprecipitation assay (RIPA) lysis buffer. A bicinchoninic acid (BCA) protein kit (Beyotime Biotechnology, Shanghai, China) was then utilized for protein quantifications. Before being transferred to polyvinylidene fluoride (PVDF) membranes, materials were electrophoresed on a 10% SDS polyacrylamide gel (SDS-PAGE) (Merck Millipore, Billerica, MA, USA). Blocking in 5% nonfat milk and tris-buffered saline buffer (TBST), then membranes were treated with *GARS* (ab125008, Abcam, Shanghai, China), and β-actin (ab8227, Abcam) overnight at 4 ℃, after that incubated with HRP-conjugated secondary antibody (Sangon, Shanghai, China) for 1 h at 37 ℃. Enhanced chemiluminescence revealed protein bands (ECL; Beyotime) followed by analysis utilizing ImageJ software.

Quantitative real-time polymerase chain reaction (QRT-PCR)

Following manufacturer instructions, total RNA was isolated utilizing TRIzol reagent (Invitrogen), dissolved in RNA-free H_2O, and frozen at –80 ℃. Each 1 μg RNA sample was utilized to synthesize cDNA utilizing Reverse Transcriptase Kit (Thermo, Waltham, MA, USA). Afterward, qPCR utilizing an SYBR Green PCR kit (Thermo) was carried out on a real-time detector (ABI, Carlsbad, MA, USA). *GARS* had the following primer sequences:primer F, 5'-AGTGCTGCTTAGAGGTGCTC-3', primer R, 5'-CCTGGGAGTAATCACAATGC 5–3'. Expression data were computed utilizing the $2^{-\Delta\Delta Ct}$ technique and normalization was performed using GAPDH as an internal reference for relative expression level control. *Tables 1*,*2* illustrate the patients information for PCR.

Extracellular vesicle isolation

Cells and other debris were separated out of the collected

Table 1 Information about samples analyzed for cancer and paracancerous GARS differences

ID	Type	Gender	Age (years)	Grade	T	N	M
594042	BC tissue	Male	71	Low	1	0	0
597966	BC tissue	Male	69	High	1	0	0
597685	BC tissue	Female	73	High	2	2	0
594042	Paracancerous tissue	Male	71	Low	1	0	0
597966	Paracancerous tissue	Male	69	High	1	0	0
597685	Paracancerous tissue	Female	73	High	2	2	0

All three pairs of samples were obtained from patients after total cystectomy, none of whom had received preoperative drug therapy. Externally normal mucosa was taken as paracancerous tissue for analysis. BC, bladder cancer.

Table 2 Information about samples analyzed for urine EV extraction and further analysis

ID	Type	Gender	Age (years)	Grade	T	N	M	Group
598669	BC	Male	55	High	2	0	0	High GARS
538760	BC	Female	75	High	3	0	0	High GARS
595913	BC	Male	81	High	3	1	0	High GARS
595068	BC	Female	81	High	2	0	0	High GARS
594661	BC	Male	78	High	1	0	0	High GARS
536866	BC	Male	69	High	2	1	0	High GARS
579977	BC	Male	51	High	4	0	0	Low GARS
592726	BC	Male	75	High	3	0	0	Low GARS
568725	BC	Male	76	High	2	0	0	Low GARS
591632	BC	Male	81	High	1	0	0	Low GARS
587748	BC	Male	43	High	2	0	0	Low GARS
598458	BC	Male	87	High	1	0	0	Low GARS
697669	ccRCC	Male	55	Low	1b	0	0	High GARS
638760	ccRCC	Female	75	High	2a	0	0	High GARS
694913	ccRCC	Male	81	High	3a	1	0	High GARS
695068	ccRCC	Female	81	Low	2a	0	0	High GARS
696661	ccRCC	Male	78	Low	1a	0	0	High GARS
636866	ccRCC	Male	69	Low	2b	1	0	High GARS
692726	ccRCC	Male	75	Low	3a	0	0	Low GARS
663725	ccRCC	Male	76	Low	2b	0	0	Low GARS
691532	ccRCC	Male	81	High	1b	0	0	Low GARS
686748	ccRCC	Male	43	Low	2a	0	0	Low GARS
699458	ccRCC	Male	87	High	1b	0	0	Low GARS
697566	ccRCC	Male	69	Low	1b	0	0	Low GARS

All samples were divided into high and low groups according to the expression of GARS in tissues, and EVs were extracted from patients' urine and the expression level of GARS was measured. EV, extracellular vesicle; BC, bladder cancer; ccRCC, clear cell renal carcinoma.

urine and centrifuged at 1,000 L for 15 min. The Exoquick extracellular vesicle precipitation solution (System Biosciences, Palo Alto, CA, USA) was utilized for the isolation of extracellular vesicles. *Table 2* illustrates the patients information for urine extracellular vesicle extraction.

Cell Counting Kit-8 (CCK-8)

CCK-8 (APExBIO, Houston, TX, USA) was utilized to assess cell proliferation. About 3×10^3 target cells were planted into each well of a 96-well culture plate and kept at 37 ℃ for one night. Cells were exposed to CCK-8 (10 µL/well) and incubated for 2 h after being transfected at 24, 48, 72, and 96 h. Then, at 450 nm, the optical densities of all the wells were measured.

Wound healing assays

Cells were inoculated in six-well plates, and after 24 h, 200 µL pipetting head was used to scratch the cells in the plate, and the serum-free medium was changed. By running a plastic tip across single-layered cells, wounds were created. The time of wound infliction was considered as 0 h, and the wounds were photographed under a microscope with an attached digital camera after 0, 12, and 24 h. ImageJ 1.48 v quantified the percentage of migrating cell-covered areas. Triplicates of all experiments were done to ensure accuracy.

Transwell invasion assay

Transwell chambers have been used to conduct invasion tests with and without Matrigel (Corning, Kennebunk, USA). While 5×10^4 cells were planted in 300 µL of serum-free media through upper chamber, 700 µL of 10% FBS-media was added in lower chamber and let to incubate for 24 h. Following a 20-minute fixation in 4% formaldehyde, we gently scraped off the remaining cells in the upper chamber and gave the cells a quick rinse in phosphate buffered solution (PBS). After staining the cells for 10 min with 0.1% crystal violet in 1 mL/well, the wells were rinsed triplet with PBS to void any residual stain. Through the use of a 200× microscope, the total number of migrating or invading cells may be determined.

Tumor xenograft experiments

We divided 10 mice into two groups: a control group and a knockdown group. Subcutaneously implant tumor cells into the left abdomen of nude mice to establish a xenograft model. Monitor the size of the tumor every 5 days. Tumor volume = (length × Width^2)/2.

Statistical analysis

R 4.1.2 and GraphPad Prism 9.3.0 was utilized to conduct all statistical analyses. The Kolmogorov-Smirnov test determined whether to apply a parametric or non-parametric rank-based analysis. The Fisher exact and Wilcoxon rank-sum tests were applied to categorical and continuous variables, respectively, to test hypotheses. Survival analysis estimation was conducted using Kaplan-Meier and Cox regression multivariate analysis, and group comparisons were made utilizing a log-rank test. A cluster profiler package was utilized to determine GO enrichment terms and KEGG pathways. Two groups of data satisfying normal distribution were tested by *t*-test otherwise using Mann-Whitney *U* test. P value <0.05 was regarded significant, for all statistical analysis. *, P<0.05; **, P<0.01; ***, P<0.001.

The affiliation shown in the animal experiment ethical approval being inconsistent with the authors' affiliation was mainly due to the change of the corresponding author's unit from the Second Hospital of Tianjin Medical University to the General Hospital of Tianjin Medical University.

Results

GARS is highly expressed in BC and is associated with poor prognosis

With the assistance of the shiny online platform, which incorporates sequencing data from TCGA and the GTEx database, we first assessed *GARS* expression in 33 different cancer types. Interestingly, 32 of 33 cancer types exhibited considerably greater levels of *GARS* expression in tumor tissue, whereas in the sarcomatoid carcinoma (SARC), the *GARS* expression levels of the tumor and normal tissues were similar. *GARS* was highly expressed in most tumor tissues, supporting its oncogene function (*Figure 1A*). We further validated that *GARS* was markedly overexpressed in BC compared to corresponding normal tissue using the TCGA database (*Figure 1B*).

GARS is associated with poor prognosis

Kaplan-Meier survival curves discovered that patients in the *GARS*-high group had a poor prognosis, with high *GARS*

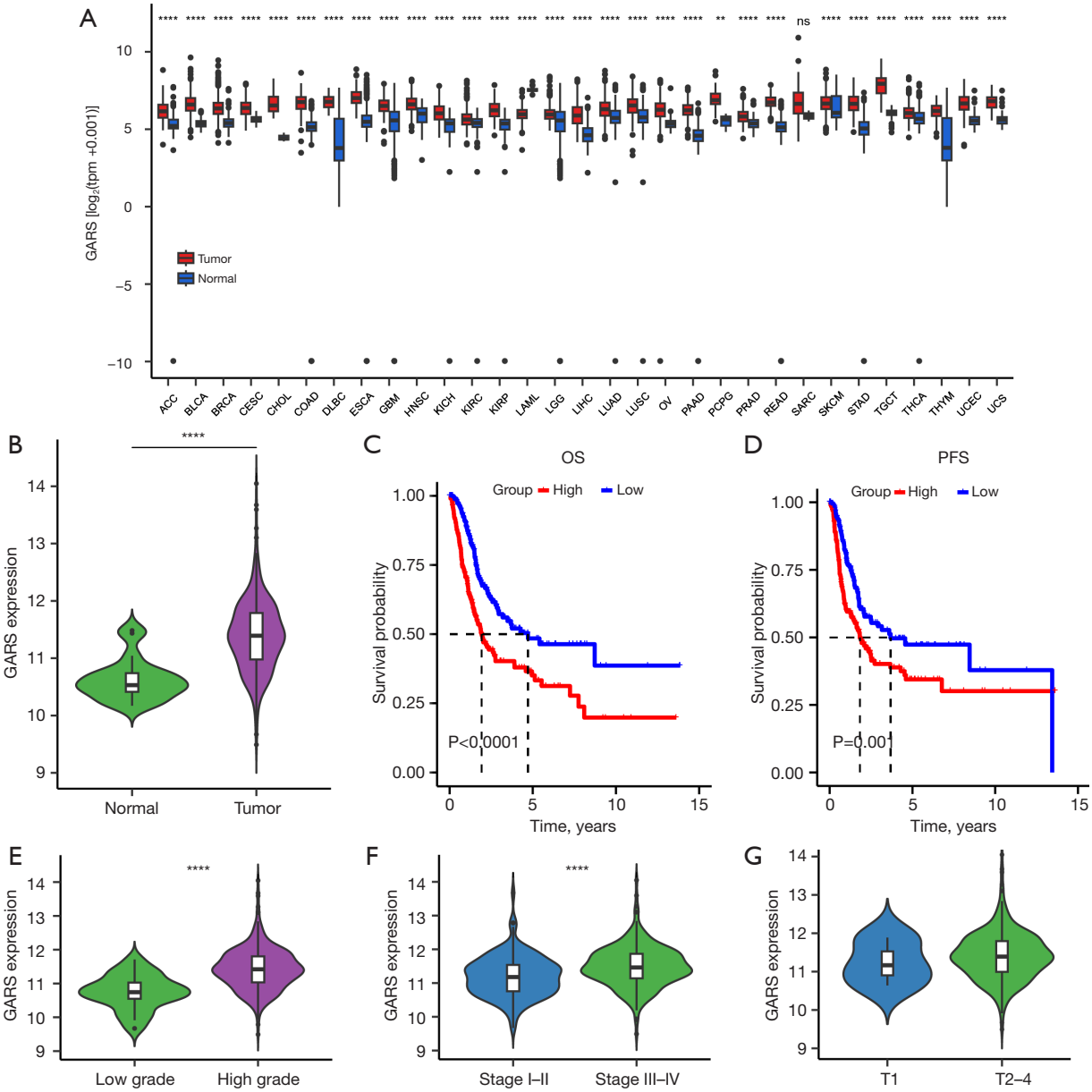

Figure 1 Correlation between *GARS* and bladder cancer. (A) *GARS* expression in pan-cancer. (B) TCGA database showed high expression of *GARS* in bladder cancer. (C,D) Bladder cancer patients with low *GARS* expression had better OS and PFS. (E-G) Relationship between *GARS* and clinical characteristics of bladder cancer. **, P<0.01; ***, P<0.001; ****, P<0.0001; ns, P>0.05. TCGA, The Cancer Genome Atlas; OS, overall survival; PFS, progression-free survival.

expression leading to shorter OS and PFS in BC patients (*Figure 1C,1D*). Additionally, we examined the relationship between *GARS* expression and the clinical characteristics of BC. Not surprisingly, *GARS* expression showed a significant positive correlation with tumor grade and stage (*Figure 1E-1G*). The above findings implied that *GARS* was a trustworthy biomarker and was most likely implicated in the development of BC. We then used univariate and multivariate Cox regression to investigate if the *GARS* expression was an independent predictor of the BC patient's prognosis. The analysis indicated that *GARS* was a prognostic indicator independent of certain other clinical characteristics (*Figure 2A,2B*). Moreover, receiver operating characteristic (ROC) curve and decision curve analysis

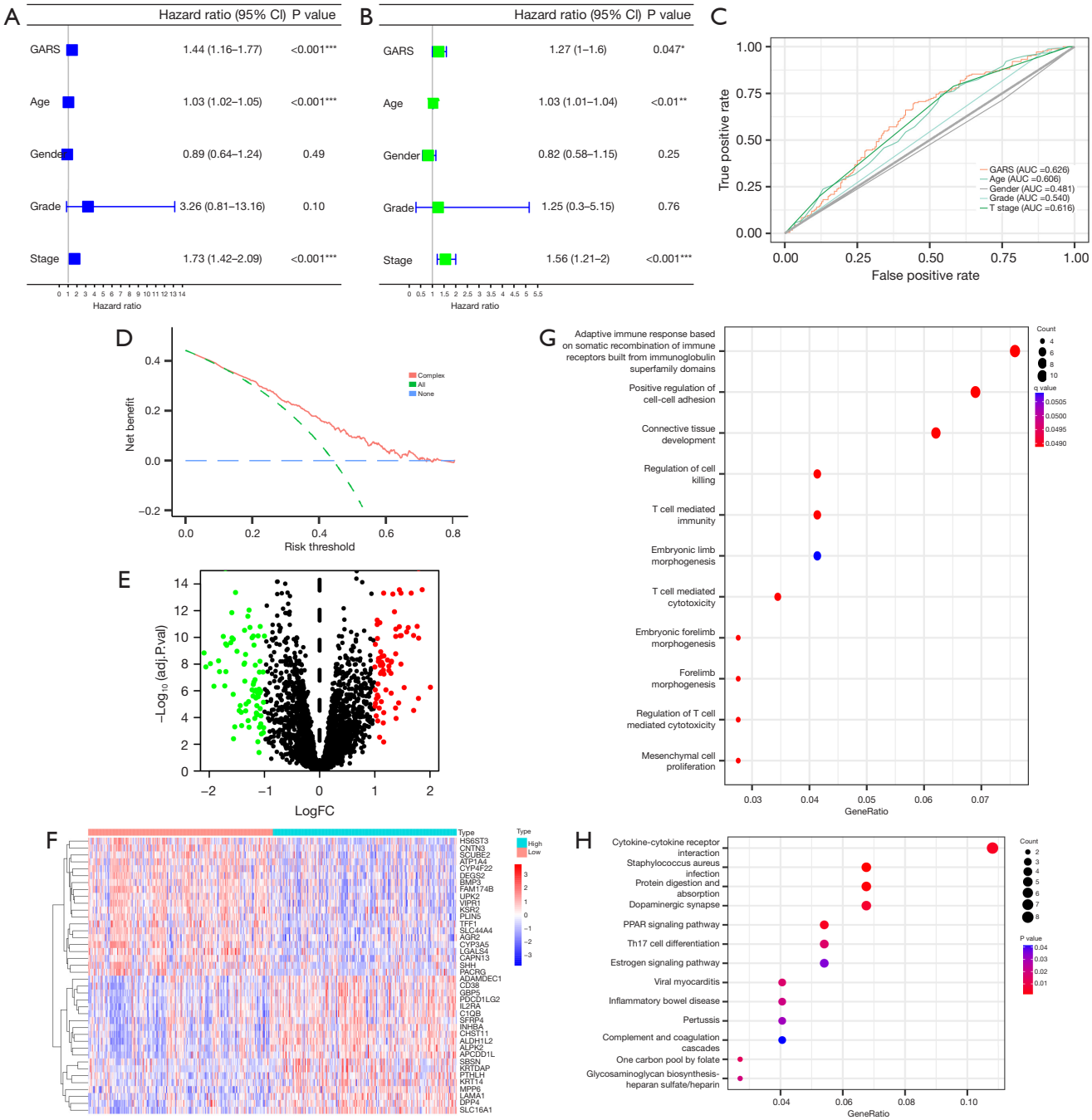

Figure 2 *GARS* is an independent prognostic factor for patients with bladder cancer and its potential biological function. (A,B) Univariate and multifactorial COX analyses showed that *GARS* is an independent prognostic factor for patients with bladder cancer. (C,D) Receiver operating characteristic and decision curve analysis curves suggested *GARS* can be used to predict 5-year survival in bladder cancer patients. (E) The Cancer Genome Atlas samples were divided into two groups of high and low expression by median *GARS* expression for differential gene analysis. Red dots represent highly expressed genes in the *GARS* high expression group and green dots represent lowly expressed genes in the *GARS* high expression group. Black dots indicate undifferentiated genes. (F) Top 20 differential genes between high and low expression groups. (G,H) Differential genes enrichment analysis. *, P<0.05; **, P<0.01; ***, P<0.001. CI, confidence interval; FC, fold change; AUC, area under the curve.

(DCA) curve depict that *GARS* expression has superior prognostic prediction ability for BC patients compared to traditional tumor staging (*Figure 2C*,*2D*). Similarly *GARS* was validated as BC-independent post factor in GSE13507 (Figure S1).

Functional analysis of GARS

To further investigate the biological role of *GARS* in BC, we separated BC patients into *GARS*-high and *GARS*-low groups based on the median value of *GARS* expression, and then we compared the differentially expressed genes (DEGs) between the two groups. The genes that differ most between the two groups are displayed on the heatmap (*Figure 2E*,*2F*).

We noticed that some biomarkers were significantly highly expressed in the *GARS*-high group. For example, Shh signaling promotes tumorigenicity and stem cell generation by stimulating EMT in BC (12). We further carried out functional enrichment analysis on DEGs between *GARS*-high and *GARS*-low groups. GO analysis revealed the DEGs enriched in immune-related pathways (*Figure 2G*), like adaptive immune response based on somatic recombination of immune receptor built from immunoglobulin superfamily domains, regulation of cell killing, T cell mediated immunity and regulation of T cell mediated cytotoxicity, were significantly enriched in these DEGs. Moreover, KEGG analysis uncovered that these DEGs were significantly enriched in TH17 differentiation and cytokine-cytokine receptor interaction. Thus, *GARS* predominantly regulates immune cell infiltration in BC (*Figure 2H*). Additionally, these DEGs displayed enrichment of peroxisome proliferators-activated receptors (PPAR) signaling pathways, suggesting that *GARS* may be involved in the regulation of tumor lipid metabolism.

GARS is linked to tumor immune infiltration

We further analyzed the correlation between *GARS* expression and immune cell infiltration scores. The findings revealed that the majority of immune cell infiltration was positively linked with *GARS* expression, including active B cell, activated CD4 T cell, activated CD8 T cell, immature B cell, macrophage, effector memory CD8 T cell, natural killer (NK) cell and Treg cells, etc. (*Figure 3*).

However, when we calculated the degree of immune checkpoint expression, we found that many immune checkpoints, including PD1, PDL1, TIGIT, TIM3 and CTLA4, were significantly overexpressed in *GARS*-high group (*Figure 4A*). Despite having a high level of immune infiltration, patients in the *GARS*-high group may have inadequate anti-tumor status because of the high expression of immunological checkpoints, according to our observation. Patients in the *GARS*-high group may achieve a high response rate during immunotherapy.

The mutation landscape of GARS and tumor stemness analysis

We assessed the somatic mutation rate in the *GARS*-high and *GARS*-low groups due to the oncogenic role of *GARS* in BC. Somatic mutations occurred in 379 of 405 patients in BC. Patients in the *GARS*-high group had considerably higher rates of *P53* and Titin (*TTN*) mutations than those in the *GARS*-low group (*Figure 4B*). *TP53* is a tumor suppressor gene that is mutated in more than half of all human cancers. Tumors with *P53* mutations progress more rapidly and have a poorer prognosis (13). *P53* mutations are more frequent in *GARS*-high patients, suggesting that *GARS* is connected to the P53 pathway. We also investigated the connection between the *GARS* expression and the tumor stem cell score.

Growing evidence indicates that increased expression of stemness-related biomarkers in tumor cells is highly correlated with drug resistance, cancer recurrence, and tumor proliferation (14). Then, we assessed the correlations of the DNAss and RNAss with *GARS* (*Figure 4C*,*4D*). The results indicated that *GARS* was positively correlated with RNAss. Finally, we calculated the concentration causing a 50% reduction growth (IC50) of drugs to determine which drugs have significantly different sensitivities between *GARS*-high and *GARS*-low groups. Patients in the *GARS*-high group had a higher sensitivity to cisplatin, epirubicin, vinblastine, and paclitaxel (*Figure 5*).

GARS is enriched in myofibroblasts in the TME and promotes the transition of NMIBC to MIBC by participating in EMT.

More and more studies have demonstrated that the microenvironment plays an important role in tumor development (15-18). To further investigate the biological functions of *GARS*, we categorized 23,519 cells into 9 clusters, which were classified as T/NK cells, epithelial cells, macrophages, myofibroblasts, plasma cells, B cells and endothelial cells according to the cell markers shown in *Table 3* (*Figure 6A-6C*). Myofibroblast transformation refers to a characteristic phenotypic transformation of local

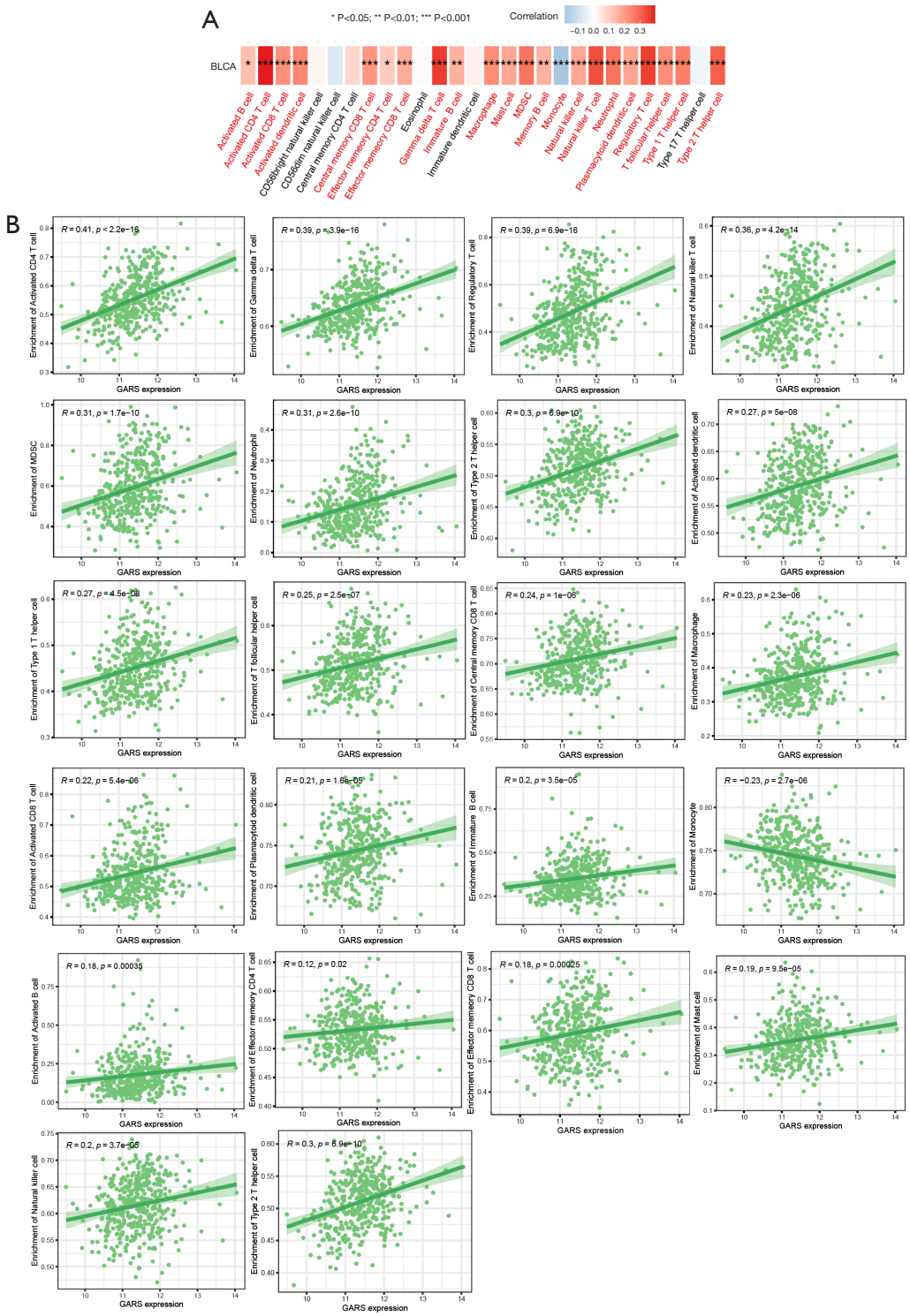

Figure 3 Exploration of tumor immune microenvironment between high *GARS* group and low *GARS* group. (A) Single-sample gene set enrichment analysis demonstrated *GARS* is associated with the immune microenvironment in bladder cancer. (B) Demonstration of statistically different results in (A) via scatterplots.

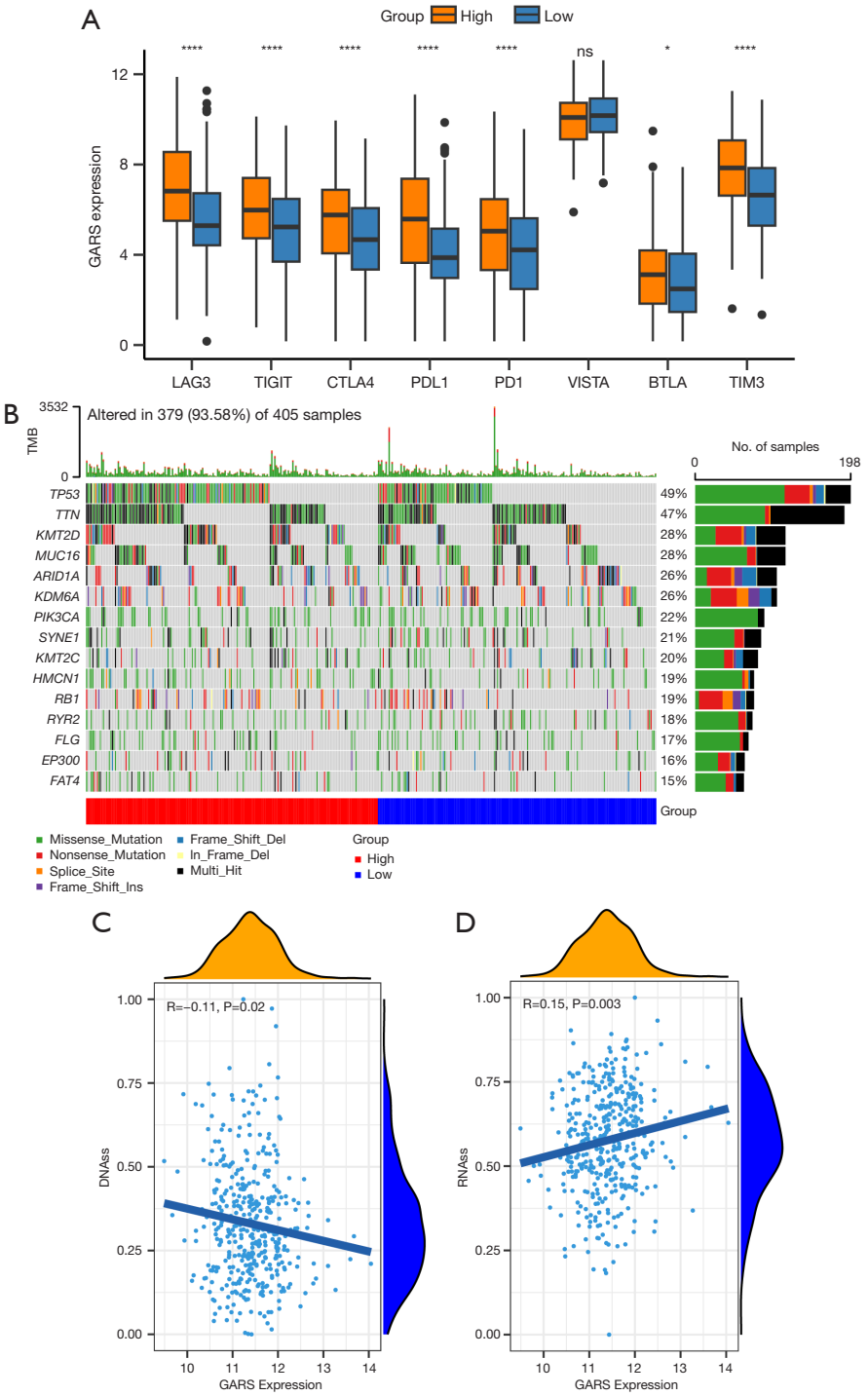

Figure 4 Analysis of *GARS* with tumor stem cell score, mutation and differential expression of immune-related checkpoints. (A) The expression of immune-related checkpoints among high and low *GARS* groups. (B) The mutation landscape of *GARS*. (C,D) The relationship between *GARS* and DNA stemness score and RNA stemness score. *, P<0.05; ****, P<0.0001; ns, P>0.05. TMB, tumor mutational burden.

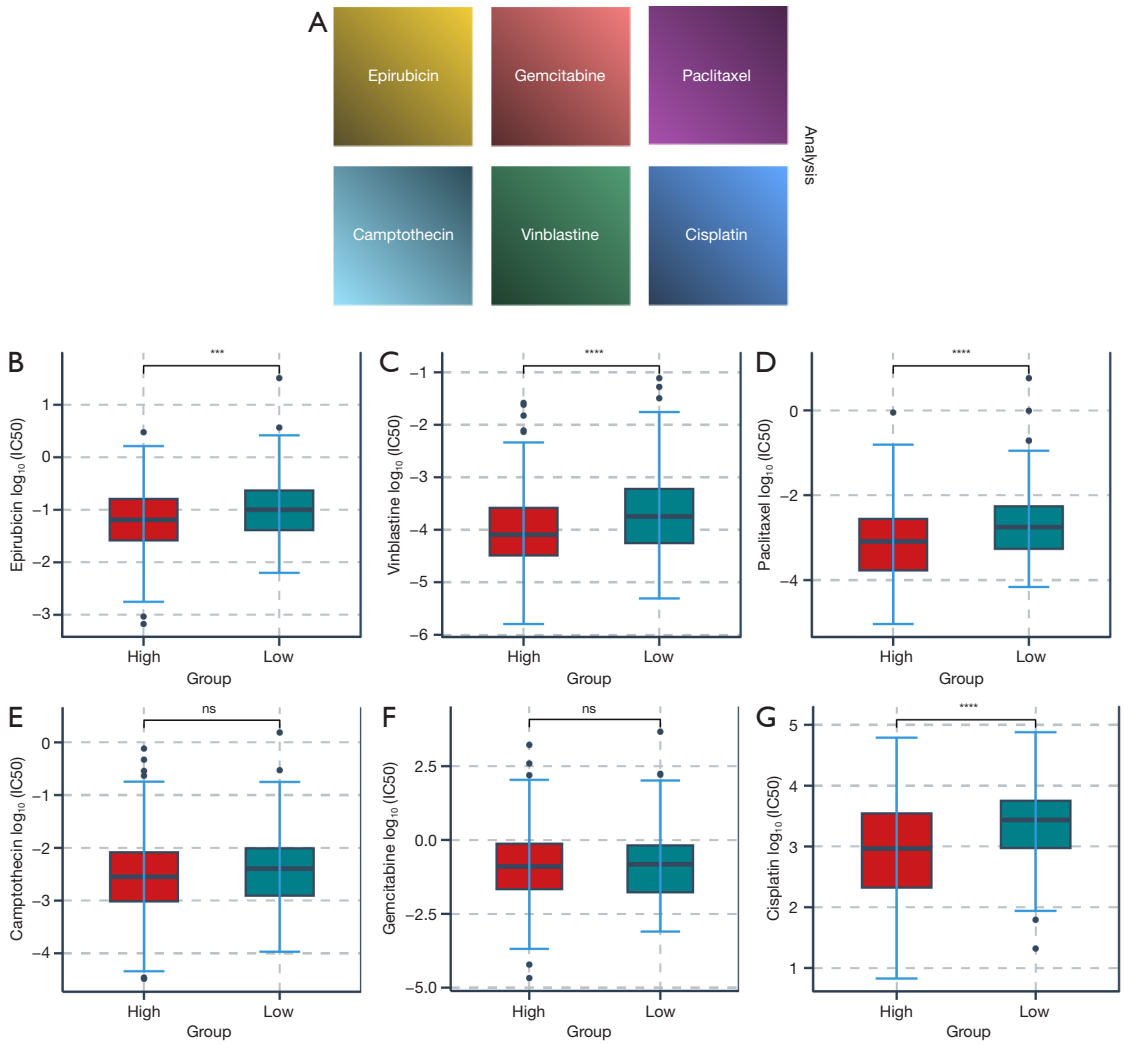

Figure 5 (A) Common chemotherapy drugs used to treat bladder cancer. (B-G) The difference of multiple anti-cancer drugs sensitivity between high GARS group and low GARS group. Y-axis represents the log10 (IC50) of the drug. ***, P<0.001; ****, P<0.0001; ns, P>0.05. IC50, half-maximal inhibitory concentration.

Table 3 Cell markers

Cell	Marker
T/NK cell	CD2, CD3D, CD3E, CD3G, CD4, CD8A, CD8B, NKG7, CD56, GNLY
Myofibroblasts	ATCA2, TAGLN, PDGFRA, PDGFRB
Epithelial cell	EPCAM, KRT8, KRT1, KRT10
B cell	CD19, MS4A1, CD79B, CD79A
Macrophages	AIF1, CSF1R, TYROBP, FCER1G, LYZ, CST3, PTPRC, MS4A6A, CD68, CD1E, IL3RA, LAMP3
plasma cell	TNFRSF17, CD38, IGHG1, IGHG4, IGHG, MZB1
Endothelial cell	CDH5, ENG, CLDN5, CD31, PECAM1

NK, natural killer.

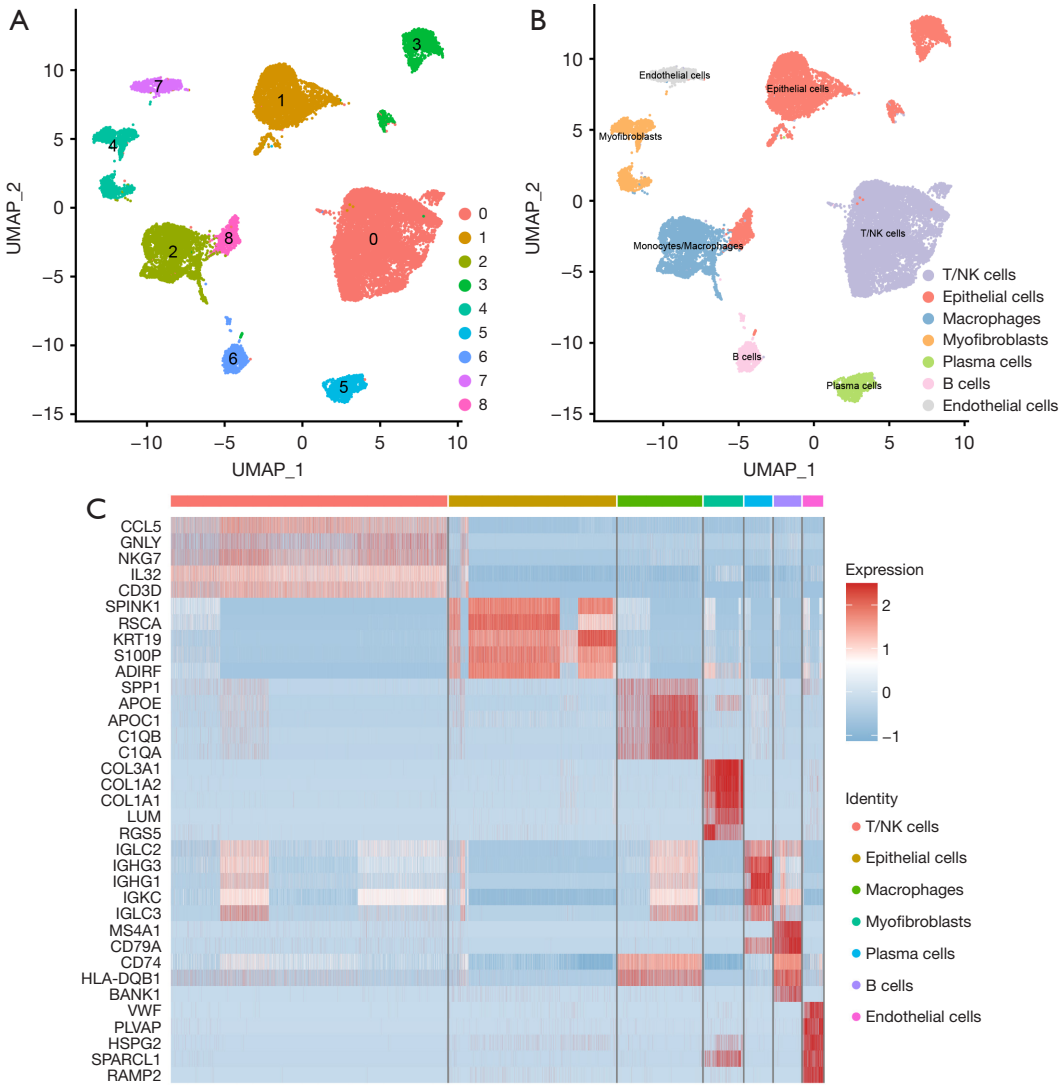

Figure 6 Cell-type classification in bladder cancer. (A) UMAP plot of 9 cell clusters. (B) UMAP plot exhibiting the cell types in bladder cancer. The X-axis and Y-axis represent the new low-dimensional coordinates extracted from the original high-dimensional data by the UMAP algorithm. They no longer represent specific features in the original data, but rather the location of the data points in the new coordinate system after dimensionality reduction. (C) Heatmap of the top five marker genes in each cell cluster. UMAP, uniform manifold approximation and projection; NK, natural killer.

fibroblasts, epithelial cells, or bone marrow mesenchymal stem cells migrating to the site of injury under the action of environmental factors of injury, and the special pathologic mesenchymal cells that undergo this transformation are called myofibroblasts (19). Myofibroblasts are seldom found in adult normal tissues, and they are mainly seen in tumors, tissue repair, and other pathological states, which have an important influence on the development of tumor cells, and are a key evolutionary process during tumor progression (20). In this study, we found that *GARS* was enriched in myofibroblasts (*Figure 7A*), in addition to epithelial cells, in microenvironment. In the previous enrichment analysis, we observed that *GARS* and its related genes were functionally enriched in the positive regulation of cell-cell adhesion (*Figure 2G*). Following these findings, we explored the relationship between *GARS* and five EMT-related genes and were surprised to find that *GARS* was positively correlated with the expression of CCL2, EGR1,

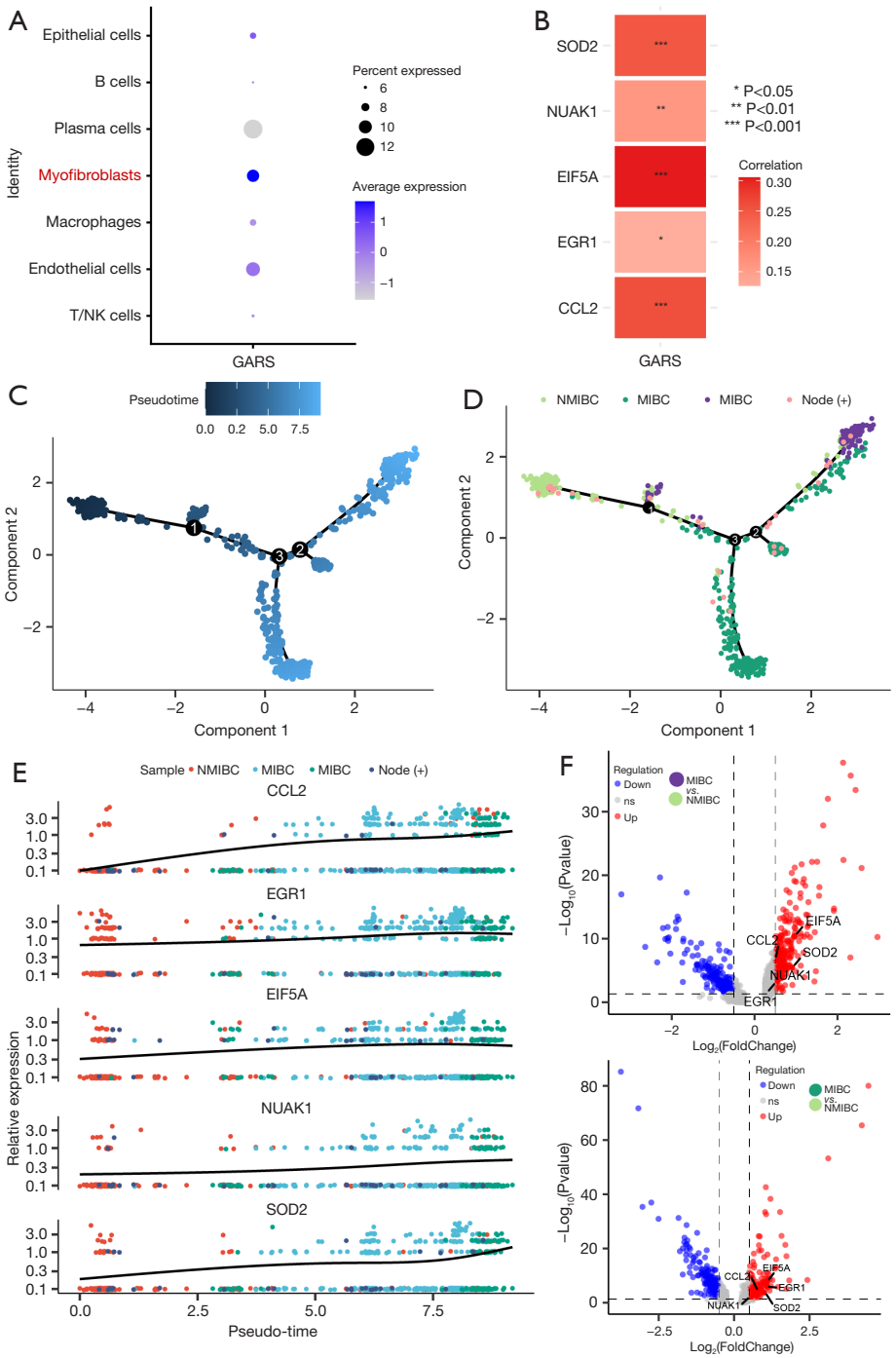

Figure 7 *GARS* is mainly enriched in myofibroblasts in the microenvironment and is associated with EMT. (A) Distribution of *GARS* in various cell types. (B) *GARS* was positively associated with five EMT-related genes in the TCGA database. A differentiation trajectory of T cells, colored based on pseudotime (C) and cell type (D) is shown. So as the five EMT-related genes (E). (F) Volcano plot demonstrating differential genes between NMIBC and MIBC. EMT, epithelial-mesenchymal transition; TCGA, The Cancer Genome Atlas; NMIBC, non-muscle invasive bladder cancer; MIBC, muscle invasive bladder cancer.

EIF5A, NUAK1 and SOD2 (*Figure 7B*). Furthermore, we mapped the myofibroblast differentiation trajectory by utilizing the Monocle2 R package (*Figure 7C*). Notably, the trajectory clearly demonstrated the progression of BC from non-muscle invasion to muscle invasion, and during the progression from NMIBC to MIBC (*Figure 7D*), we could clearly see the gradual increase in the expression of CCL2, EGR1, EIF5A, NUAK1 and SOD2 (*Figure 7E*), and the expression of the above five genes was higher in MIBC than in NMIBC (*Figure 7F*). This suggested that *GARS* may have influenced the process of EMT by participating in the biological processes of these five genes, leading to the progression of NMIBC toward MIBC.

GARS enhances proliferation and invasion of BC cells

To further explore the biological function of *GARS* in BC, we used 2 *GARS*-specific shRNA to make *GARS* knockdown cells in T24 and 5637 cell lines (*Figure 8A*). The expression of *GARS* was significantly decreased in T24 and 5637 cells both at mRNA and protein level. CCK-8 assay showed that silencing of *GARS* using si*GARS*-1 and si*GARS*-2 significantly reduced the viability of T24 and 5637 cells (*Figure 8B*). Wound healing assay and Transwell results showed that all the proliferation and invasion ability of T24 and 5637 cells were decreased after silencing *GARS* (*Figure 8C,8D*). In addition, Xenograft tumours from respective groups were depicted following injection with si*GARS* T24 cells and T24 cells, confirmed the tumorigenic effects of *GARS in vivo* (*Figure 8E*).

Expression of GARS in urological tumors tissues and uEVs

Kidney is known to contribute a lot uEVs to urine, more than bladder in some donor groups (21). To further explore the prognostic role of *GARS* plays in BC patients, we added clear cell renal carcinoma (ccRCC) patients as reference. We characterized extracellular vesicles isolated from the urine of BC patients, ccRCC patients and healthy individuals (*Figure 9A*). The result of RT-PCR showed there was no significant difference between the expression of *GARS* in the uEVs of ccRCC patients with high expression of *GARS* and the uEV of ccRCC patients with low expression of *GARS* (*Figure 9B*). We performed RT-PCR to detect the expression of *GARS* in the uEV of BC patients. We were surprised to find that *GARS* expression was significantly higher in extracellular vesicles of BC patients compared with normal subjects, and the level of *GARS* expression in uEVs was also high in the *GARS* high expression group (*Figure 9C*). GARS protein expression information was obtained from THPA, and the results showed that *GARS* remained highly expressed at the protein level, in BC (*Figure 9D*).

Discussion

BC is the most common and aggressive cancer of the urinary system (22). The standard treatment for MIBC is still early radical cystectomy; however, the 5-year cancer-specific mortality rate for individuals with BC has not decreased significantly, highlighting the surgical approach's shortcomings (23). First-line chemotherapy regimens have relatively high objective response rates of 36–65% for individuals with advanced BC. However, their 5-year OS is only 13–15%, indicating that chemoresistance will emerge in almost all patients as the cancer advances (24). Patients with advanced cancer who do not respond to first-line chemotherapy have a very dismal prognosis, and there are no effective treatment choices (25). With the advent of immune checkpoint inhibitors and the availability of targeted medicines in recent years, BC treatment has seen considerable advancements. Nevertheless, only PD-1/PD-L1 inhibitors, FGFR3 inhibitors, and antibody-drug conjugates (ADCs) are currently approved by the FDA for the treatment of advanced/metastatic uroepithelial carcinoma in patients who are platinum-refractory or platinum-ineligible (26). We still lack particular therapeutic targets for BC despite the fact that high-throughput sequencing has increased the finding of molecular targets and enhanced our knowledge of their cellular effects. Hence, in order to develop precision medicine, researchers need to dedicate themselves to investigating the molecular mechanisms of BC and identifying new targets for its therapy. Previous studies have demonstrated that *GARS* is a potential oncogene that is associated with poor OS in a variety of cancers (27). For instance, by regulating the mTOR signaling system, *GARS* accelerates the proliferation, cell cycle, migration, and invasion of breast cancer cells (28). Importantly, Chen *et al.* demonstrated that *GARS* is a reliable urinary biomarker in uroepithelial carcinoma (29). In prostate cancer cell lines, *GARS* knockdown reduces cell motility and invasion and causes S-phase cell arrest and early apoptotic signals (5). However, the biological function and biomarker role of *GARS* in BC have not been studied. In our work, we identified that *GARS* was a reliable biomarker for BC patients and could

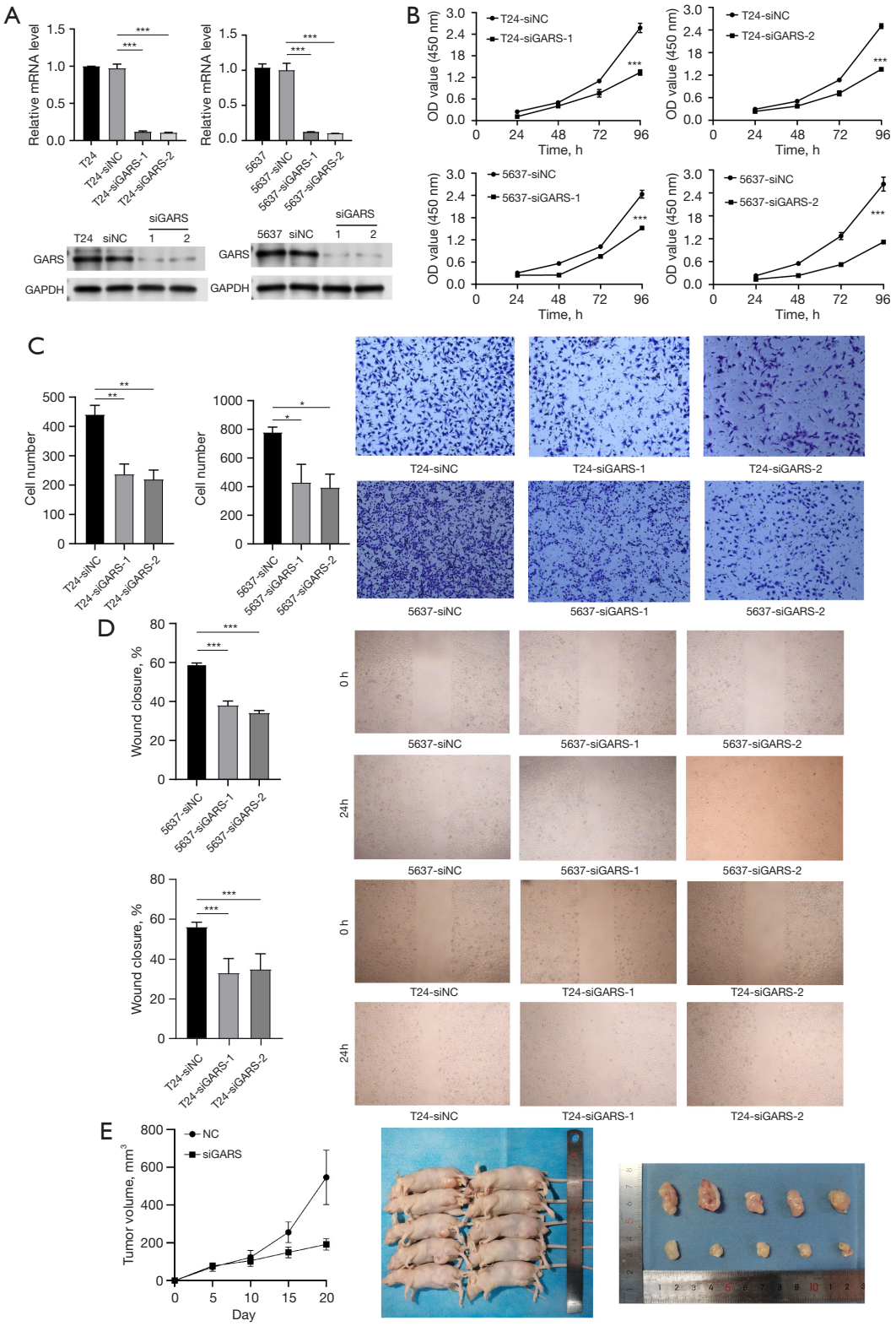

Figure 8 *GARS* knockdown can effectively reduce the proliferation and invasion of bladder cancer cells. (A) *GARS* was stably silenced in T24 cells and 5637 cells by transfection and selection, respectively. *GARS* expression was confirmed by real-time PCR and western blotting

analysis. (B) CCK-8 assays revealed that down-regulation of *GARS* inhibited the growth rate of T24 and 5637 cells. (C,D) Wound healing assay and transwell results showed that all the proliferation and invasion ability of T24 and 5637 cells were decreased after silencing *GARS* (crystal violet staining, the magnification of C was 400×, magnification of D was 100×). (E) Xenograft tumours from respective groups were depicted following injection with siGARS T24 cells and T24 cells. All images were processed using image J, and specific data were obtained for statistical analysis after setting thresholds. *, P<0.05; **, P<0.01; ***, P<0.001; ns, P>0.05. CCK-8, Cell Counting Kit-8; PCR, polymerase chain reaction.

accurately predict the BC patient's prognosis. Furthermore, *GARS* participated in tumor immune infiltration and was associated with immunotherapy efficacy. In order to confirm the role of *GARS* in modulating tumour cell fate, *GARS* was knocked down in BC cell lines. The results demonstrated *GARS* significantly promoted cell proliferation and invasion *in vitro*. In addition, found that *GARS* was highly expressed in the uEVs of BC and the trend was consistent with the trend of *GARS* expression in tissues.

First, we evaluated the *GARS*'s mRNA expression value in 33 cancers using TCGA and GTEx databases. *GARS* was highly expressed in almost all cancer tissues, implying that it may play a role in the development of multiple cancers. Next, we demonstrated that *GARS* was also highly expressed in BC tissues using the TCGA database, suggesting a promising future for *GARS* in BC diagnosis. Additionally, OS and PFS survival analyses all revealed that *GARS* was significantly associated with BC patient's prognosis. Elevated *GARS* expression resulted in poorer prognosis. To some extent, tumor grading and clinical staging can show how tumors progress. Our results showed that *GARS* expression was positively correlated with grade and stage of BC patients. According to the above findings, *GARS* might have an important role in the prognosis of BC patients, and it plays a role in the TME.

Then, compared the DEGs between the *GARS*-high and *GARS*-low groups and found that these DEGs were mainly enriched in immune-related pathways, including adaptive immune response based on somatic recombination of immune receptor built from immunoglobulin superfamily domains, regulation of cell killing, T cell mediated immunity and regulation of T cell mediated cytotoxicity, TH17 cell differentiation and cytokine-cytokine receptor interaction. Furthermore, by examining the somatic mutations in BC patients, patients in the *GARS*-high category had significantly greater rates of *P53* and *TTN* mutations than those in the *GARS*-low subgroup. Patients with high *GARS* had a higher prevalence of *P53* mutations, indicating that *GARS* was involved in the P53 pathway.

Meanwhile, single cell analysis confirmed that *GARS* was not only expressed in epithelial cells but also significantly expressed in macrophages and T cells. The results presented above imply that *GARS* is involved in controlling the tumor immune microenvironment. The TME refers to the complex and heterogeneous multicellular environment in which tumors grow. TME includes stromal cells, numerous cytokines, and immune cells such as T and B lymphocytes, TAM, NK cells, and others. It is now commonly acknowledged that TME plays a crucial role in dynamically controlling the development of cancer and affecting treatment outcomes, and therapeutic strategies targeting the TME have emerged as a promising approach to cancer treatment (30). In addition, the TME is associated with poor prognosis and treatment resistance, including immunotherapy (31). The clinical potential of immunotherapy may be significantly limited by immunosuppression microenvironment, according to a growing body of research (32). BC is a disease with a unique TME consisting of immune cells, cytokines, and a rich pattern of immune gene expression, making it an ideal candidate for immunotherapy treatment (33). We discovered the majority of immune cell infiltration was positively linked with *GARS* expression, including active B cell, activated CD4 T cell, activated CD8 T cell, immature B cell, macrophage, effector memory CD8 T cell, NK cell and Treg cells, etc. In contrast, high *GARS* expression may result in less infiltration of monocytes. The key immune cells for anti-tumor immunity are NK cells and activated CD8 T cells, whereas Treg cells produce a tumor immunosuppressive environment. *GARS* was significantly associated with multiple immune cell infiltrates, suggesting a complex role in the immune microenvironment. Notably, we found that most of immune check points, including PD1, PDL1, TIGIT, TIM3 and CTLA4, were significantly overexpressed in *GARS*-high group. Due to the strong expression of immunological checkpoints, patients in the *GARS*-high group may not have enough anti-tumor status while having a high level of immune infiltration. Patients in the *GARS*-high category may receive an immunotherapy with a high response rate. In HCC, the investigators

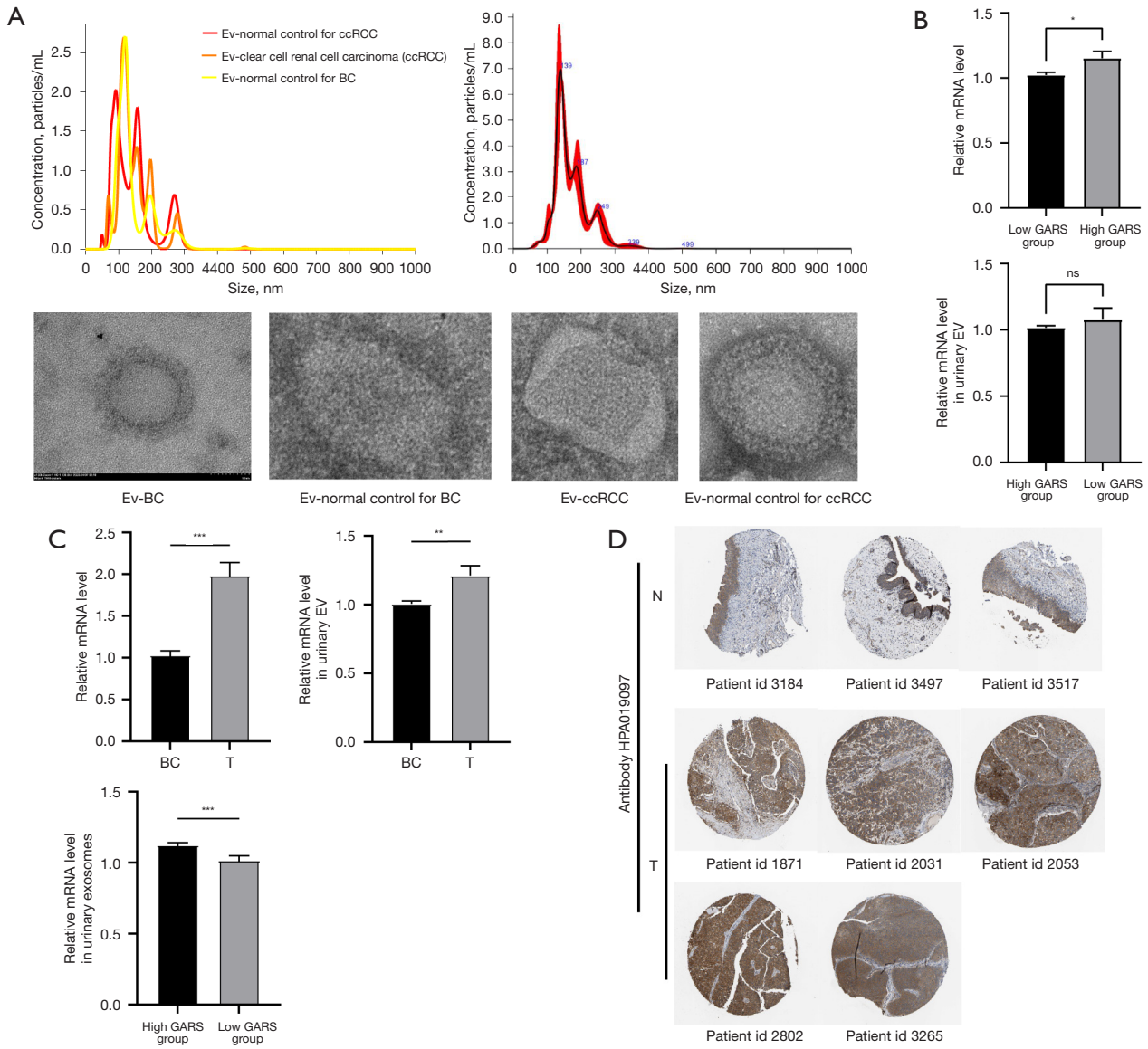

Figure 9 Expression of *GARS* in urological tumors tissues and urinary extracellular vesicles. (A) Extraction of exosomes from the urine of normal subjects, patients with bladder cancer, and patients with ccRCC. The magnification of A was 80kx. The camera type used in (A) was sCMOS, camera level: 14 (NTA 3.0 Levels). The data were further analyzed using NANOSIGHT. (B) Distinguishing the high GARS group from the low GARS group in ccRCC patients' tissues. And RT-PCR validated high expression of GARS in urinary extracellular vesicles from ccRCC patients. (C) RT-PCR validated high expression of *GARS* in BC patients' tissues. And RT-PCR validated high expression of *GARS* in urinary extracellular vesicles from BC patients. Patients with high *GARS* expression in BC tissues had similarly *GARS* expression tend in urinary extracellular vesicles. (D) Immunohistochemical images in The Human Protein Atlas database show high expression of *GARS* in BC. The link for *GARS* levels are provided for BC tissues (https://www.proteinatlas.org/ENSG00000106105-*GARS*1/pathology/urothelial+cancer#ihc) and individual normal tissues (https://www.proteinatlas.org/ENSG00000106105-*GARS*1/tissue/urinary+bladder). *, P<0.05; **, P<0.01; ***, P<0.001; ns, P>0.05. ccRCC, clear cell renal carcinoma; RT-PCR, real-time polymerase chain reaction; BC, bladder cancer.

confirmed that *GARS* overexpression promoted tumor growth and enhanced infiltration of $CD206^+$ TAMs *in vivo*, which was consistent with the results of our study (6).

In addition, we further explored the role of *GARS* in the TME using GSE211388 and we found that in addition to epithelial cells, *GARS* was enriched in myofibroblasts. Myofibroblasts have been found to have the following roles during tumor progression: (I) maintaining tumor cells, secreting a large number of soluble cytokines to promote tumor cell proliferation, synthesizing a large amount of extracellular matrix, and constituting a metabolic system suitable for tumor cell growth (34); (II) providing morphological scaffolds, assembling tumor cells, constructing tumor tissues, and promoting spatial development of tumor tissues (35); (III) enabling tumor cells to shed and gain invasive migration through epithelial mesenchymal transformation (36); (IV) secretion of vascular endothelial growth factor, promoting the proliferation of microvessels and microlymphatic vessels, increasing the permeability of blood vessels and lymphatic vessels, ensuring the nutrient supply of tumor cells and assisting the entry of tumor cells into the vascular system etc. (37).

As for clinical BC samples, in NMIBC, E-cadherin expression was slightly diminished, and the expression of both SOX2 and NANOG was negligible. In contrast, in MIBC, E-cadherin expression was highly and heterogeneously diminished, while the expression of both SOX2 and NANOG was increased. This signifies an upward trend in EMT levels during the progression of NMIBC to MIBC (38).

We identified five genes (*CCL2*, *EGR1*, *EIF5A*, *NUAK1* and *SOD2*) positively associated with EMT among the differential genes in the progression of NMIBC toward MIBC. In triple-negative breast cancer, M2-like TAMs promote EMT in triple negative breast cancer (TNBC) through activation of the CCL2/AKT/β-catenin signaling pathway (39). Meanwhile, CCL2/CCR2 activation can promote EMT in prostate cancer (40). Wang *et al.* demonstrated EGR1 induces EMT via a P300/SNAI2 pathway in pancreatic cancer (41). In contrast, in gastric cancer, downregulation of EGR1 leads to suppression of EMT levels (42). Besides, EGR1-CCL2 feedback loop might exert critical roles on EMT and angiogenesis of chemoresistant gastric cancer (43). Xu *et al.* showed that down-regulation of EIF5A-2 prevents EMT in non-small-cell lung cancer cells (44). In non-small-cell lung cancer, EIF5A-2 regulates EMT, which causes tumor invasion and metastatic disease. When it comes to NUAK1, Guan *et al.* indicated that the knockdown of NUAK1 may inhibit prostate cancer cells EMT, migration and invasion (45). And increased expression of NUAK1 in HCC cells through the ceRNA network enhances the ability of mesenchymal transition of epithelial cells, which promotes HCC migration and invasion (46). As for SOD2, RUNX2 promotes EMT and bone metastasis in breast cancer by inhibiting the expression of PPARα and SOD2 (47). In addition to this, we found a positive correlation between *GARS* and the expression of these five genes in database. In order to investigate the role of *GARS* in myofibroblasts during the progression of BC from NMIBC to MIBC, we did a proposed pseudotime analysis to simulate the progression from NMIBC to MIBC. We were surprised to find that the expression of the five EMT-related genes gradually increased as the BC progressed, suggesting that *GARS* regulates EMT in myofibroblasts during the progression from NMIBC to MIBC. In conclusion, *GARS* plays a complex role in regulating the tumor immune microenvironment.

Beyond what has been mentioned above, we performed *GARS* knocked down in BC cell lines. The results showed that *GARS* significantly promoted cell proliferation and invasion *in vitro* and *vivo*. In addition, found that *GARS* had higher expression levels in uEVs of BC patients. extracellular vesicles are nanoscale vesicles derived from endocytosis, formed by fusion of multivesicular bodies with membranes and secreted into the extracellular matrix or body fluids. Extracellular vesicles play an important role in the diagnosis and prognostic markers of the disease (48). To further investigate the significance of *GARS* in uEVs, we divided 12 patients into two groups based on median *GARS* expression level and found that patients with high *GARS* also had higher expression of *GARS* in uEVs. This suggests that we can measure *GARS* in uEVs instead of tissues to predict the prognosis of patients.

Conclusions

In sum, bioinformatics analysis was performed to confirm that *GARS* is a potential biomarker and oncogene for BC that can accurately predict the cancer patient's prognosis. Furthermore, we identified that *GARS* is mainly involved in regulating immune cell infiltration in BC and investigated its relationship with immune checkpoints. Besides, also found that *GARS* is enriched in myofibroblasts in the TME in BC and affects the progression from NMIBC to MIBC

by participating in the regulation of EMT. In addition, *GARS* promotes the proliferation and invasion of BC, and its detection in uEVs may replace the detection in tissues to better assess the prognosis of patients. This is similar to the findings of Chen *et al.* (29). In conclusion, *GARS* may be a promising biomarker and therapeutic target for immunotherapy in BC.

Acknowledgments

Funding: This study was supported by the Science and Technology Project of Tianjin Health Committee (No. ZC20116).

Footnote

Reporting Checklist: The authors have completed the MADR reporting checklist. Available at https://tcr.amegroups.com/article/view/10.21037/tcr-23-2148/rc

Data Sharing Statement: Available at https://tcr.amegroups.com/article/view/10.21037/tcr-23-2148/dss

Peer Review File: Available at https://tcr.amegroups.com/article/view/10.21037/tcr-23-2148/prf

Conflicts of Interest: All authors have completed the ICMJE uniform disclosure form (available at https://tcr.amegroups.com/article/view/10.21037/tcr-23-2148/coif). The authors have no conflicts of interest to declare.

Ethical Statement: The authors are accountable for all aspects of the work in ensuring that questions related to the accuracy or integrity of any part of the work are appropriately investigated and resolved. For human experiments: The study was conducted in accordance with the Declaration of Helsinki (as revised in 2013). The study was approved by the Medical Ethics Committee of the Second Hospital of Tianjin Medical University, Tianjin, China (KY2023K185). For animal experiments: Experiments were performed under a project license (No. JCPD20221018028) granted by Animal Ethics Committee of the Second Hospital of Tianjin Medical University, Tianjin, China (JCPD20221018028), in compliance with China animal experiments guidelines for the care and use of animals.

References

1. Bray F, Ferlay J, Soerjomataram I, et al. Global cancer statistics 2018: GLOBOCAN estimates of incidence and mortality worldwide for 36 cancers in 185 countries. CA Cancer J Clin 2018;68:394-424.
2. Lenis AT, Lec PM, Chamie K, et al. Bladder Cancer: A Review. JAMA 2020;324:1980-91.
3. Konala VM, Adapa S, Aronow WS. Immunotherapy in Bladder Cancer. Am J Ther 2022;29:e334-7.
4. Markovitz R, Ghosh R, Kuo ME, et al. GARS-related disease in infantile spinal muscular atrophy: Implications for diagnosis and treatment. Am J Med Genet A 2020;182:1167-76.
5. Khosh Kish E, Gamallat Y, Choudhry M, et al. Glycyl-tRNA Synthetase (GARS) Expression Is Associated with Prostate Cancer Progression and Its Inhibition Decreases Migration, and Invasion In Vitro. Int J Mol Sci 2023;24:4260.
6. Wang J, Yang B, Wang D, et al. GARS is implicated in poor survival and immune infiltration of hepatocellular carcinoma. Cell Signal 2022;94:110302.
7. Zhang X, Dong W, Zhang J, et al. A Novel Mitochondrial-Related Nuclear Gene Signature Predicts Overall Survival of Lung Adenocarcinoma Patients. Front Cell Dev Biol 2021;9:740487.
8. Xu N, Yao Z, Shang G, et al. Integrated proteogenomic characterization of urothelial carcinoma of the bladder. J Hematol Oncol 2022;15:76.
9. Subramanian A, Tamayo P, Mootha VK, et al. Gene set enrichment analysis: a knowledge-based approach for interpreting genome-wide expression profiles. Proc Natl Acad Sci U S A 2005;102:15545-50.
10. Vento-Tormo R, Efremova M, Botting RA, et al. Single-cell reconstruction of the early maternal-fetal interface in humans. Nature 2018;563:347-53.
11. Sun H, Huang Q, Huang M, et al. Human CD96 Correlates to Natural Killer Cell Exhaustion and Predicts the Prognosis of Human Hepatocellular Carcinoma.

Hepatology 2019;70:168-83.
12. Islam SS, Mokhtari RB, Noman AS, et al. Sonic hedgehog (Shh) signaling promotes tumorigenicity and stemness via activation of epithelial-to-mesenchymal transition (EMT) in bladder cancer. Mol Carcinog 2016;55:537-51.
13. Bykov VJN, Eriksson SE, Bianchi J, et al. Targeting mutant p53 for efficient cancer therapy. Nat Rev Cancer 2018;18:89-102.
14. Walcher L, Kistenmacher AK, Suo H, et al. Cancer Stem Cells-Origins and Biomarkers: Perspectives for Targeted Personalized Therapies. Front Immunol 2020;11:1280.
15. Xiao Y, Yu D. Tumor microenvironment as a therapeutic target in cancer. Pharmacol Ther 2021;221:107753.
16. Bader JE, Voss K, Rathmell JC. Targeting Metabolism to Improve the Tumor Microenvironment for Cancer Immunotherapy. Mol Cell 2020;78:1019-33.
17. Ho WJ, Jaffee EM, Zheng L. The tumour microenvironment in pancreatic cancer - clinical challenges and opportunities. Nat Rev Clin Oncol 2020;17:527-40.
18. de Visser KE, Joyce JA. The evolving tumor microenvironment: From cancer initiation to metastatic outgrowth. Cancer Cell 2023;41:374-403.
19. Xiao X, Huang C, Zhao C, et al. Regulation of myofibroblast differentiation by miR-424 during epithelial-to-mesenchymal transition. Arch Biochem Biophys 2015;566:49-57.
20. O'Connor JW, Gomez EW. Cell adhesion and shape regulate TGF-beta1-induced epithelial-myofibroblast transition via MRTF-A signaling. PLoS One 2013;8:e83188.
21. Blijdorp CJ, Hartjes TA, Wei KY, et al. Nephron mass determines the excretion rate of urinary extracellular vesicles. J Extracell Vesicles 2022;11:e12181.
22. Antoni S, Ferlay J, Soerjomataram I, et al. Bladder Cancer Incidence and Mortality: A Global Overview and Recent Trends. Eur Urol 2017;71:96-108.
23. Vlachostergios PJ, Faltas BM. Treatment resistance in urothelial carcinoma: an evolutionary perspective. Nat Rev Clin Oncol 2018;15:495-509.
24. Liu S, Chen X, Lin T. Emerging strategies for the improvement of chemotherapy in bladder cancer: Current knowledge and future perspectives. J Adv Res 2022;39:187-202.
25. Yafi FA, North S, Kassouf W. First- and second-line therapy for metastatic urothelial carcinoma of the bladder. Curr Oncol 2011;18:e25-34.
26. Morales-Barrera R, Suárez C, González M, et al. The future of bladder cancer therapy: Optimizing the inhibition of the fibroblast growth factor receptor. Cancer Treat Rev 2020;86:102000.
27. Jiang Y, Ouyang W, Zhang C, et al. Prognosis and Immunotherapy Response With a Novel Golgi Apparatus Signature-Based Formula in Lung Adenocarcinoma. Front Cell Dev Biol 2022;9:817085.
28. Li X, Sun H, Liu Q, et al. Conjoint analysis of circulating tumor cells and solid tumors for exploring potential prognostic markers and constructing a robust novel predictive signature for breast cancer. Cancer Cell Int 2021;21:708.
29. Chen CJ, Chou CY, Shu KH, et al. Discovery of Novel Protein Biomarkers in Urine for Diagnosis of Urothelial Cancer Using iTRAQ Proteomics. J Proteome Res 2021;20:2953-63.
30. Bejarano L, Jordão MJC, Joyce JA. Therapeutic Targeting of the Tumor Microenvironment. Cancer Discov 2021;11:933-59.
31. Binnewies M, Roberts EW, Kersten K, et al. Understanding the tumor immune microenvironment (TIME) for effective therapy. Nat Med 2018;24:541-50.
32. Xiang X, Wang J, Lu D, et al. Targeting tumor-associated macrophages to synergize tumor immunotherapy. Signal Transduct Target Ther 2021;6:75.
33. Nair SS, Weil R, Dovey Z, et al. The Tumor Microenvironment and Immunotherapy in Prostate and Bladder Cancer. Urol Clin North Am 2020;47:e17-54.
34. Castells M, Milhas D, Gandy C, et al. Microenvironment mesenchymal cells protect ovarian cancer cell lines from apoptosis by inhibiting XIAP inactivation. Cell Death Dis 2013;4:e887.
35. Hirokawa Y, Yip KH, Tan CW, et al. Colonic myofibroblast cell line stimulates colonoid formation. Am J Physiol Gastrointest Liver Physiol 2014;306:G547-56.
36. Liu C, Chen F, Han X, et al. Role of TGF-β1/p38 MAPK pathway in hepatitis B virus-induced tubular epithelial-myofibroblast transdifferentiation. Int J Clin Exp Pathol 2014;7:7923-30.
37. Cho JA, Park H, Lim EH, et al. Exosomes from breast cancer cells can convert adipose tissue-derived mesenchymal stem cells into myofibroblast-like cells. Int J Oncol 2012;40:130-8.
38. Migita T, Ueda A, Ohishi T, et al. Epithelial-mesenchymal transition promotes SOX2 and NANOG expression in bladder cancer. Lab Invest 2017;97:567-76.
39. Chen X, Yang M, Yin J, et al. Tumor-associated macrophages promote epithelial-mesenchymal transition and the cancer stem cell properties in triple-negative

breast cancer through CCL2/AKT/β-catenin signaling. Cell Commun Signal 2022;20:92.
40. Shen T, Li Y, Wang D, et al. YAP1-TEAD1 mediates the perineural invasion of prostate cancer cells induced by cancer-associated fibroblasts. Biochim Biophys Acta Mol Basis Dis 2022;1868:166540.
41. Wang Y, Qin C, Zhao B, et al. EGR1 induces EMT in pancreatic cancer via a P300/SNAI2 pathway. J Transl Med 2023;21:201.
42. Zhao J, Geng L, Duan G, et al. REC8 inhibits EMT by downregulating EGR1 in gastric cancer cells. Oncol Rep 2018;39:1583-90.
43. Yan J, Gao Y, Lin S, et al. EGR1-CCL2 Feedback Loop Maintains Epithelial-Mesenchymal Transition of Cisplatin-Resistant Gastric Cancer Cells and Promotes Tumor Angiogenesis. Dig Dis Sci 2022;67:3702-13.
44. Xu GD, Shi XB, Sun LB, et al. Down-regulation of eIF5A-2 prevents epithelial-mesenchymal transition in non-small-cell lung cancer cells. J Zhejiang Univ Sci B 2013;14:460-7.
45. Guan Y, Shi H, Xiao T. NUAK1 knockdown suppresses prostate cancer cell epithelial-mesenchymal transition, migration, and invasion through microRNA-30b-5p. Int J Clin Exp Pathol 2018;11:5694-704.
46. Chu DX, Jin Y, Wang BR, et al. LncRNA HOTAIR Enhances Epithelial-to-mesenchymal Transition to Promote the Migration and Invasion of Liver Cancer by Regulating NUAK1 via Epigenetic Inhibition miR-145-5p Expression. J Cancer 2023;14:2329-43.
47. Yin X, Teng X, Ma T, et al. RUNX2 recruits the NuRD(MTA1)/CRL4B complex to promote breast cancer progression and bone metastasis. Cell Death Differ 2022;29:2203-17.
48. Urabe F, Kosaka N, Ito K, et al. Extracellular vesicles as biomarkers and therapeutic targets for cancer. Am J Physiol Cell Physiol 2020;318:C29-39.

Cite this article as: Chen K, Chen S, Wu S, Sun G, Jiang Y, Liu R. Prognostic value of GARS in bladder cancer and its role in the tumor microenvironment. Transl Cancer Res 2024;13(6):2825-2846. doi: 10.21037/tcr-23-2148

